The influence of burr formation and feed rate on the fatigue life of drilled titanium and aluminium alloys used in aircraft manufacture

Abdelhafeez, Ali M.; Soo, Sein Leung; Aspinwall, David K.; Dowson, Anthony; Arnold, Dick

DOI:
10.1016/j.cirp.2018.03.013

Document Version
Peer reviewed version

Citation for published version (Harvard):
Abdelhafeez, AM, Soo, SL, Aspinwall, DK, Dowson, A & Arnold, D 2018, 'The influence of burr formation and feed rate on the fatigue life of drilled titanium and aluminium alloys used in aircraft manufacture', *CIRP Annals*, vol. 67, no. 1, pp. 103-108. https://doi.org/10.1016/j.cirp.2018.03.013

Contents lists available at SciVerse ScienceDirect

CIRP Annals Manufacturing Technology

Journal homepage: www.elsevier.com/locate/cirp

The influence of burr formation and feed rate on the fatigue life of drilled titanium and aluminium alloys used in aircraft manufacture

Ali M. Abdelhafeez [a,1], Sein Leung Soo (1)[a,*], David K. Aspinwall (1)[a], Anthony Dowson [b], Dick Arnold [c]

[a] *Machining Research Group, Department of Mechanical Engineering, School of Engineering, University of Birmingham, Edgbaston, Birmingham, B15 2TT, UK*
[b] *Airbus Operations Ltd., Pegasus House, Aerospace Avenue, Filton, Bristol BS34 7PA, UK*
[c] *Mapal Ltd., Old Leicester Road, Rugby CV21 1DZ, UK*

[1] Currently at Rolls-Royce University Technology Centre (UTC) in Manufacturing and On-Wing Technology, University of Nottingham

Following drilling, fatigue life trials were performed on as-drilled and deburred specimens made from Ti-6Al-4V, AA7010 and AA2024, with feed rates varied at 2 levels. Deburring dramatically increased the fatigue performance of the Ti-6Al-4V and AA7010 samples by 69% and 283% respectively, but there was no significant effect on the AA2024 alloy. Fractography showed failure initiated near the exit burrs in Ti-6Al-4V and AA7010 specimens but not in the AA2024 workpieces. Correlation (R^2) of fatigue notch factor against the sum of entrance and exit burr height was 0.68 and 0.79 for Ti-6Al-4V and AA7010 respectively, compared to 0.54 for AA2024.

Deburring; Fatigue; Fracture analysis

1. Introduction

Carbon fibre reinforced plastic (CFRP) composites now account for the majority of weight in modern civil aircraft structures (~50% of Boeing 787), with more traditional titanium and aluminium alloys liable for ~35% of the overall weight [1]. Many of the critical load bearing sections of the fuselage and wings consist of hybrid composite-metallic assemblies which require the drilling of high tolerance holes for mechanical joining [2]. The integrity of such joints is a critical consideration and substantial research has been undertaken relating to the effect of drilling operations on fatigue performance. The majority of work has focussed on the influence of hole machining marks/scoring, surface roughness and residual stress [3-6], with only limited studies devoted to evaluating burr formation on fatigue behaviour. Results from comprehensive trials performed by Koster el al. [7] involving 7.93 mm diameter tapered interference-fit fastener holes in AA7175-T73511 aluminium alloy, indicated that the presence of exit burrs up to ~0.5 mm high had no detrimental influence on the fatigue life of the joint, as none of the associated failures initiated in the burred region. Work by Noronha et al. [8] to assess the fatigue performance of drilled and reamed fastener holes (6.35 mm diameter) in AA7475-T7351, similarly concluded that burrs had no discernible impact on specimen fatigue behaviour, as no cracks were observed to originate from the burrs.

Nishimura [9] investigated the effect of burrs (fabricated by milling) on the fatigue performance of Ti-6Al-4V specimens having holes drilled at diameters of 1, 2, 5 and 10 mm. The burrs were found to significantly reduce fatigue life by up to two orders of magnitude compared with corresponding non burred specimens, but only in test pieces with small diameter holes (1 and 2 mm). For specimens with larger holes (5 and 10 mm diameter), no major degradation in fatigue life was observed as peak stress caused by the burr decreased with increasing hole size. In an evaluation of drilled and reamed AA2024-T3 open hole specimens (4 mm diameter), Lanciotti and Polese [10] showed that deburring enhanced the workpiece run-out fatigue strength by ~34%. Work by Barter et al. [11] provides reinforcement for this stance based on inspection of a wide range of post service metallic airframe components from both commercial and military aircraft, to ascertain the types of manufacturing induced discontinuities/defects that initiated fatigue failure. One of the examples highlighted included a poorly deburred fastener hole, which was identified as the source of fatigue cracks in a decommissioned AA7075-T6 wing spar.

It is likely that the conflicting results detailed in the literature regarding the effect of burrs on the fatigue life of drilled components is in part due to the large variation in workpiece surface integrity and operating test conditions employed by the different researchers. The current work aimed to examine the influence of burr formation and feed rate on the fatigue performance of drilled titanium and aluminium alloy specimens.

2. Experimental work

Fatigue testing was performed on a Phoenix twin-column servo-hydraulic machine having a load capacity of 100 kN with a maximum head stroke and loading frequency of 50 mm and 50 Hz respectively; see Fig. 1a. The 3 aerospace grade materials assessed were Ti-6Al-4V annealed at 800°C for 1 hour, together with 2 aluminium alloys; AA7010-T7451 and AA2024-T351 in the solution treated, water quenched and aged condition. Both of these alloys were subsequently stress relieved by controlled stretching (1.5-3%). The rectangular fatigue specimen blanks were cut from a single slab/billet of each alloy along a consistent alignment to avoid any directionality effects in the workpieces. Each side of the test samples was finish face milled (depth of cut of 0.125 mm) symmetrically to final dimensions of 150 x 17 x 7 mm (L x W x H) in order to ensure flatness and equilibrium of residual stresses. A single through hole was subsequently drilled at the centre of each test specimen on a 3-axis machining centre using 6.35 mm diameter solid WC twist drills, see Fig 1b for

sample fatigue specimens. This resulted in a theoretical stress concentration factor K_t of 2.26 for the open hole specimens. Two different feed rates were used; 0.07 and 0.14 mm/rev for the Ti-6Al-4V and 0.08 and 0.24 mm/rev for both the AA7010 and AA2024 workpieces, while cutting speed was kept constant at 10 and 50 m/min for the Ti and Al alloys respectively. The low and high feed rate levels were selected to generate large and small exit burr heights respectively based on results from a previous publication [12], which also details the drill geometries used in the present work. All holes were drilled with cutting fluid supplied externally at a flow rate of 52 l/min.

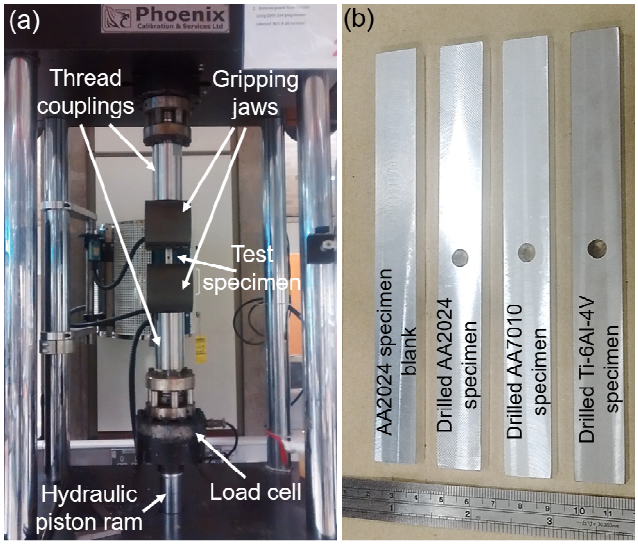

Fig. 1. (a) Fatigue test setup and (b) sample test specimens.

Tension-tension fatigue experiments were undertaken based on a standardised wing loading spectrum used by Airbus, which entailed room temperature testing at a frequency of 15 Hz and stress ratio (R) of 0.1. The free/unclamped length of the specimens held between the grips was 70 mm. Restrictions relating to fatigue machine access and workpiece material availability however precluded testing to obtain full S-N curves. As a consequence, fatigue performance in terms of the number of cycles to failure was assessed at a pre-determined load for each material based on published S-N data for a fatigue life of ~200,000 cycles (at equivalent K_t and stress ratios). The load levels utilised were 28 kN (net stress of 375.6 MPa), 14 kN (187.8 MPa) and 13 kN (174.4 MPa) for the Ti-6Al-4V [13], AA7010 [14] and AA2024 [15, 16] samples respectively. All selected loads/stresses were within 97-109% of the maximum loads employed in published fatigue data derived from flight load spectra simulation [17-19]. Test specimen preparation and loading parameters were based on fatigue testing procedures utilised by Airbus in accordance with ASTM E466 standards [20].

Trials were carried out according to the full factorial experimental array outlined in Table 1 involving two replications of each run, giving a total of 12 tests for each material. The burr height and width at hole entry and exit locations of the as-drilled specimens were measured using an Alicona InfiniteFocus G5 microscope (at 10X magnification and 0.5 µm resolution) prior to fatigue testing with results shown in Table 2. Deburring was achieved by introducing a 50 x 50 µm chamfer on both ends of the hole using a 90° countersinking tool at a feed rate and cutting speed of 0.05 mm/rev and 5 m/min respectively, with cutting fluid delivered externally. Specimens were tested to failure or up to a run out of 1 x 10^6 cycles. Fractography analysis of the failed fatigue specimens were performed using optical and scanning electron microscopy (SEM).

Table 1
Experimental array and variable factor levels for the fatigue tests.

Test	AA2024 / AA7010		Ti-6Al-4V	
	Feed rate	Hole condition	Feed rate	Hole condition
1	0.24	Deburred	0.14	Deburred
2	0.08	As-drilled	0.07	As-drilled
3	0.24	As-drilled	0.14	As-drilled
4	0.08	As-drilled	0.07	As-drilled
5	0.24	As-drilled	0.14	As-drilled
6	0.08	Deburred	0.07	Deburred
7	0.24	As-drilled	0.14	As-drilled
8	0.08	Deburred	0.07	Deburred
9	0.24	Deburred	0.14	Deburred
10	0.08	Deburred	0.07	Deburred
11	0.24	Deburred	0.14	Deburred
12	0.08	As-drilled	0.07	As-drilled

Table 2
Hole exit and entry burr height/width measurements.

Test	Exit burr height/width (µm)			Entry burr height/width (µm)		
	Ti-6Al-4V	AA7010	AA2024	Ti-6Al-4V	AA7010	AA2024
1	0/0	0/0	0/0	0/0	0/0	0/0
2	52/190	65/16	58/17	25/100	8/13	13/29
3	23/127	11/17	12/16	20/48	23/12	30/28
4	50/195	67/15	60/15	26/95	7/12	11/28
5	19/123	10/17	13/15	19/44	22/14	27/27
6	0/0	0/0	0/0	0/0	0/0	0/0
7	21/192	13/16	14/16	22/95	24/13	26/27
8	0/0	0/0	0/0	0/0	0/0	0/0
9	0/0	0/0	0/0	0/0	0/0	0/0
10	0/0	0/0	0/0	0/0	0/0	0/0
11	0/0	0/0	0/0	0/0	0/0	0/0
12	49/124	64/16	57/17	24/43	9/13	12/29

3. Results and discussion

3.1. Fatigue performance evaluation

The influence of hole condition on the number of cycles to failure at the specified stress levels for each of the workpiece materials drilled at high and low feed rates are shown in Figs. 2 and 3 respectively. Samples with deburred holes generally exhibited superior fatigue life compared to the corresponding as-drilled workpieces, although differences in performance were observed depending on the drilling feed rate and specimen material. For trials involving holes drilled at the high feed rate level, the average number of cycles to failure of the deburred Ti-6Al-4V, AA7010 and AA2024 specimens were ~69%, 190% and 8% higher respectively than the as-drilled counterparts. Similarly when drilling with the low feed rate level, deburring improved the mean number of cycles to failure of the Ti-6Al-4V, AA7010 and AA2024 open hole samples by ~48%, 283% and 93% respectively. A major factor contributing to the lower fatigue life of the as-drilled specimens was the presence of defects including microcracks and spalling/chipping at the entrance/exit regions of the holes, similar to those shown in Fig. 4, which detail sample SEM micrographs of internal hole exit burr surfaces drilled in AA2024 and Ti-6Al-4V at low feed rate levels. Such flaws can act as areas of stress concentration (due to sharp geometrical variations) and fatigue crack initiation sites, thereby accelerating failure of the specimens. In addition, the mechanism of burr formation is primarily due to plastic deformation of uncut material and is therefore generally strain hardened. Although work hardened material typically possess higher yield strength, associated ductility is generally lower compared to the initial undeformed material, leading to a lower threshold in plastic strain to failure. These conditions tend to promote cracking (and

hence fatigue initiation sites), rather than plastic deformation of the burr when under the influence of elevated stress levels.

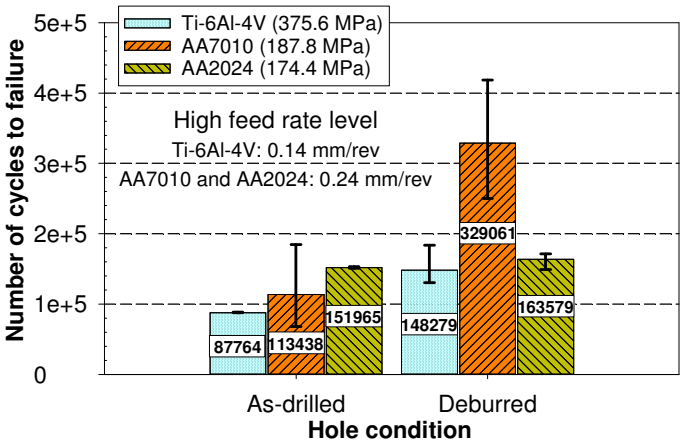

Fig. 2. Number of cycles to failure for specimens drilled at high feed rate.

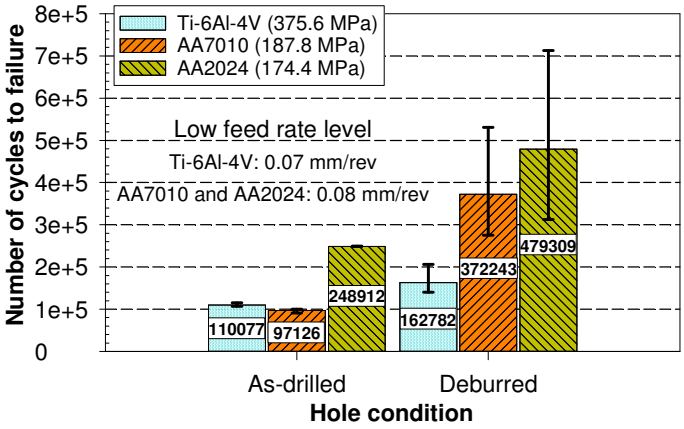

Fig. 3. Number of cycles to failure for specimens drilled at low feed rate.

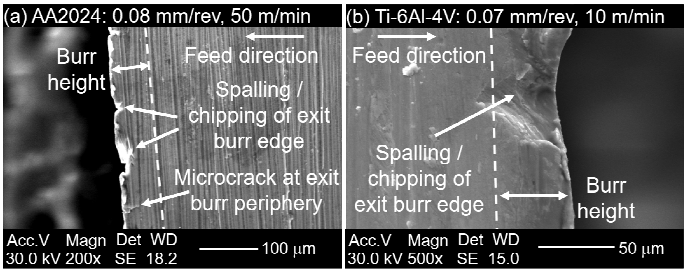

Fig. 4. Sample SEM micrographs of internal hole exit burr surfaces drilled in (a) AA2024 and (b) Ti-6Al-4V.

Compared with high feed rate results, the average number of cycles to failure was typically greater by up to ~193% for specimens drilled at low feed rate irrespective of hole condition. The exception to this was the as-drilled AA7010 specimens where fatigue life increased by ~17% when drilled at the higher feed rate level, although a comparatively larger spread of the data was observed in this case. The larger exit burrs typically obtained in the as-drilled specimens when machining at the low feed rate level did not appear to have a detrimental effect on the number of cycles to failure in the Ti-6Al-4V and AA2024 materials. A possible reason for the improved fatigue life of specimens drilled at low feed rate was the reduced hole surface roughness. Typically the average roughness for AA2024 holes varied between 0.7 and 1.0 μm Ra when drilled at low and high feed respectively, whereas for Ti-6Al-4V, the corresponding values were 0.8 and 1.4 μm Ra. Suraratchai et al. [21] concluded that differences in surface roughness was the predominant factor affecting the fatigue strength of rough and finish milled AA7010 alloy.

Statistical analysis of variance (ANOVA) was carried out to assess the significance (at the 5% level) of varying feed rate and hole condition on the mean number of cycles to failure for the 3 workpiece materials tested. For the AA7010 specimens, hole condition was the sole statistically significant factor with a percentage contribution ratio (PCR) of 73.9%. While the deburred AA2024 samples also exhibited higher mean number of cycles to failure than the as-drilled specimens, this factor was not statistically significant at the 5% level. Instead, variation in feed rate was found to be significant with a PCR of 43.4%. The comparable fatigue performance of the as-drilled and deburred AA2024 specimens and in particular those drilled at the high feed rate level, was possibly linked to the material's under-aged condition (T351) and resulting workpiece microstructure. Despite having moderate yield strength (324 MPa), the AA2024-T351 alloy is characterised by good fracture toughness and resistance to fatigue crack growth, leading to enhanced damage tolerance [22]. These mechanical properties arise from the presence of inter-granular under-aged precipitates that impede the rate of damage progression by deflecting the path of crack propagation [23], as illustrated by the schematic in Fig. 5a. This possibly outweighed the detrimental effects of burrs in the as-drilled specimens. In contrast, the AA7010 material, which was subjected to the T7451 over-aged temper condition, contained larger/harder to shear precipitates that obstruct the path of the crack, thereby forcing dislocations to 'bypass' the particles by moving around them [24], see Fig. 5b. Experimental observation of fatigue crack growth profiles in under-aged (T351) and over-aged (T7351) AA7475 aluminium alloy reported by Carter et al. [25] revealed that a saw-tooth crack path was prevalent in the former while a comparatively straight profile was seen in the latter. Additionally, the rate of fatigue crack growth of the under-aged alloy was found to be ~2000% slower than the over-aged material (at a stress intensity range ΔK of 10 MPa.m^{-2}) [25].

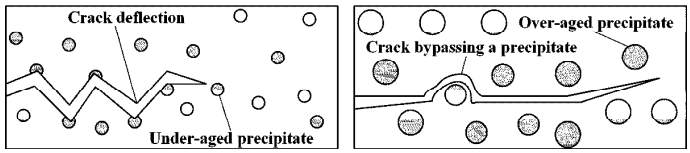

Fig. 5. Schematic showing mechanism of crack propagation in alloys processed in (a) under-aged and (b) over-aged condition.

The ANOVA for fatigue life of the Ti-6Al-4V specimens showed similar trends to the AA7010 alloy, where hole condition was a significant factor affecting the mean number of cycles to failure, and a corresponding PCR of 62.6%. According to results from finite element (FE) simulations of drilling Ti-6Al-4V reported by Abdelhafeez et al. [26], the maximum compressive residual stresses predicted at the hole surface was -500 MPa to -711 MPa when operating at feed rates of 0.07 to 0.21 mm/rev respectively. The difference in hole surface residual stress when varying feed rate from 0.07 to 0.14 m/rev was estimated to be only 14.6% based on linear interpolation. This was probably insufficient to have any marked influence on fatigue life considering the relatively high levels of compressive residual stress in both specimens. Therefore, the higher anticipated stress concentrations induced by the presence of burrs is likely to have a more pronounced effect on fatigue performance.

3.2. Specimen fractography analysis

All of the samples evaluated fractured near or along the middle plane through the centreline of the hole corresponding to the location of highest axial stress (smallest net cross sectional area) in the specimen. No visible signs of necking were observed in any of the test pieces, which suggests that the samples suffered brittle fracture (over a major part of the specimen cross section) due to fatigue crack initiation and propagation caused by the cyclic loading. Examples of failed test specimens are shown in Fig. 6.

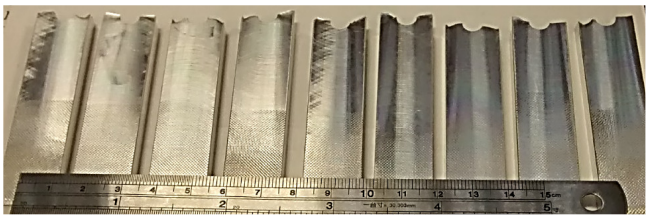

Fig. 6. Examples of failed test specimens.

Fig. 7 details optical and corresponding SEM micrographs of the fractured surfaces on AA2024 fatigue samples from selected trials. In the majority of cases, fatigue cracks initiated on the drilled surfaces towards the middle section of the hole away from the edge locations (Figs. 7a and 7c) with the exception of Test 6, where cracks occurred ~100 μm from the deburred region of the hole exit, see Fig. 7b. These observations appear to corroborate results from the previously detailed ANOVA, indicating that hole condition did not have a significant effect on the mean number of cycles to failure in AA2024 specimens.

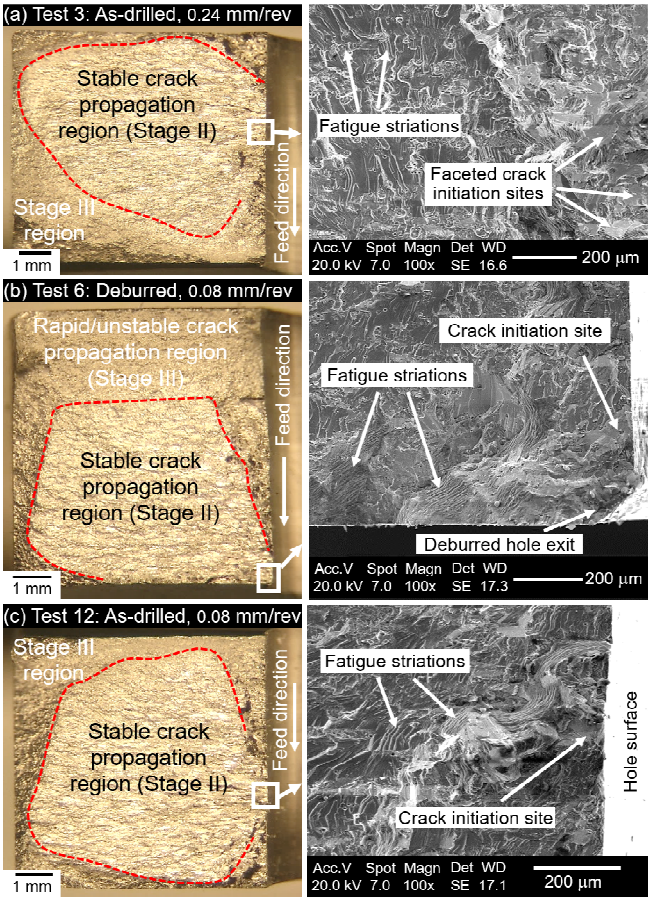

Fig. 7. Selected optical and SEM micrographs of fractured surfaces on AA2024 fatigue specimens.

Figs. 8 and 9 illustrate representative optical and SEM micrographs of fracture surfaces from selected AA7010 and Ti-6Al-4V specimens respectively. For the as-drilled samples, fatigue cracks typically originated around the vicinity of the exit burrs (Figs. 8b and 9b), while damage in the deburred specimens generally commenced at distances of ~200-390 μm from either the exit or entrance of the hole, see Figs. 8a and 9a. This suggests that the presence of burrs due to the drilling operation acted as stress concentrators, which had a substantial influence on the fatigue life of both AA7010 and Ti-6Al-4V workpiece materials. Conversely, deburring strengthened the edges and shifted the fracture initiation sites away from the entry and exit positions of the holes.

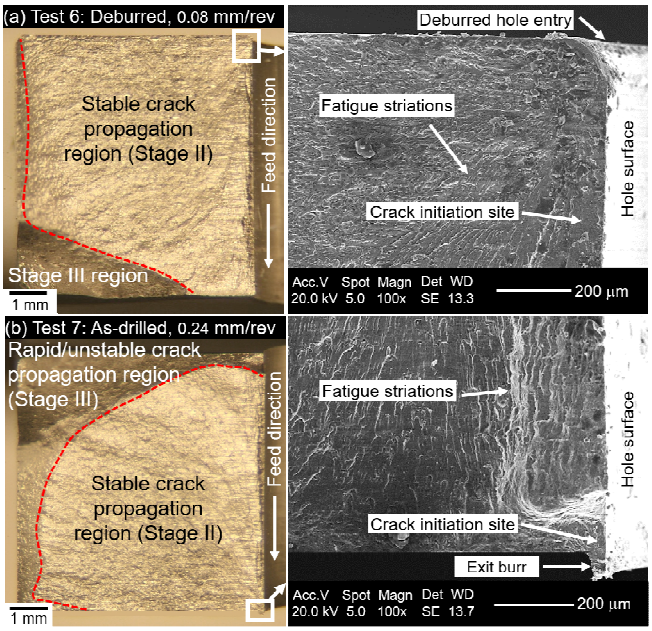

Fig. 8. Selected optical and SEM micrographs of fractured surfaces on AA7010 fatigue specimens.

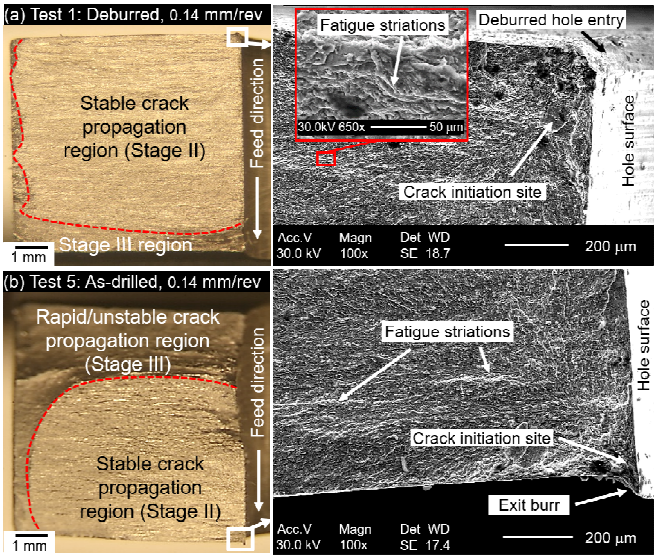

Fig. 9. Selected optical and SEM micrographs of fractured surfaces on Ti-6Al-4V fatigue specimens.

Fatigue crack initiation sites in all of the specimens were characterised by transgranular facets up to ~130 μm in size. This represents Stage I of fatigue failure and was primarily induced by localised plastic strain fields/slip bands due to the presence of

machining defects on the hole surface or burrs, rather than inherent flaws within the material. The continued application of cyclic loading led to relatively slow but stable growth/propagation of the cracks (Stage II), characterised by the 'shiny' fracture surfaces on the optical micrographs in Figs. 7-9. These were accompanied by the formation of fatigue striation marks (usually seen in most ductile alloys) generally caused by cyclic plastic blunting of the crack tip and extension during the loading cycle [24]. As the stress intensity range (ΔK) reached a critical value due to increasing crack depth, dimpled/rough fracture surfaces were observed due to void nucleation and coalescence [23]. Here, the rate of crack propagation progressed rapidly (Stage III), with certain sections of the failure surface found at an angle of ~45° to the loading direction [27].

3.3. Fatigue notch factor estimation due to burr formation

The fatigue notch factor (K_f) is a parameter normally employed to estimate the fatigue life/strength of notched components (defects acting as stress raisers). It typically has a lower value compared to the theoretical stress concentration factor (K_t) and is sensitive to the size of the notch/defect and material strength. The general definition of K_f is the ratio of the endurance limits between a notched and corresponding un-notched/smooth specimen [24]. Following the derivation of fatigue notch factors based on experimental fatigue data from Section 3.1, exponential regression was utilised to determine correlations between K_f and characteristic burr dimensions for each workpiece material.

For notched specimens subjected to cyclic loading, the mean stress at the edge of a notch (σ_{notch}) can be linked to K_f and mean stress of a smooth sample (σ_0) by Eq. (1) [24].

$$\sigma_{notch} = K_f \, \sigma_0 \tag{1}$$

The relationship between mean stress and the number of cycles to failure (N_f) can be approximated by Eq. (2) as described by Basquin [28]:

$$\sigma = A(2N_f)^b \tag{2}$$

where A and b are material empirical constants. Substituting Eq. (2) into (1) leads to:

$$K_f = \left(\frac{N_{f|notch}}{N_{f|0}} \right)^b \tag{3}$$

where $N_{f|notch}$ and $N_{f|0}$ are the number of cycles to failure for the notched and un-notched specimens respectively.

According to literature, the values of b for AA2024, AA7010 (approximated from data for AA7075) and Ti-6Al-4V are -0.126, -0.124, and -0.104 respectively [24]. In the current analysis, the deburred holes were considered as the reference un-notched specimens (fatigue life of $N_{f|0}$) and hence have a K_f value of 1. The fatigue notch factors for the as-drilled specimens (fatigue life of $N_{f|notch}$) can therefore be determined using Eq. (3) with respect to corresponding deburred specimens drilled at equivalent feed rate. The K_f values for each of the tests are detailed in Table 3.

For specimens containing multiple notches, the total stress concentration factor can be approximated as the product of the individual stress concentration factors for each notch [29]. Similarly, the overall fatigue notch factor of a drilled specimen can be estimated based on the product of the individual fatigue notch factors attributed to the entrance ($K_{f|entrance}$) and exit ($K_{f|exit}$) burrs respectively. The value of K_f is generally found to be proportional to K_t, which is commonly an exponential function of the characteristic notch dimension. By selecting burr height as the characteristic notch dimension, the overall fatigue notch factor ($K_{f|burr\ \ height}$) for a drilled specimen can therefore be reasonably assumed to be proportional to the sum of the entry ($BH_{entrance}$) and exit (BH_{exit}) burr heights. This relationship can be expressed in the form shown in Eq. (4), where A is the proportionality constant.

$$K_{f|burr\ height} = A\, e^{(BH_{entrance} + BH_{exit})} \tag{4}$$

Table 3
Fatigue notch factor values for all tests.

Test	AA7010	Ti-6Al-4V	AA2024
1	1	1	1
2	1.146	1.081	1.141
3	1.038	1.062	1.013
4	1.229	1.041	1.066
5	1.211	1.029	1.016
6	1	1	1
7	1.214	1.027	0.997
8	1	1	1
9	1	1	1
10	1	1	1
11	1	1	1
12	1.151	1.042	1.028

Fig. 10 shows regression plots for K_f values against the sum of entrance and exit burr height for each of the workpiece materials tested. The K_f for the AA7010 and Ti-6Al-4V workpieces showed reasonable correlation to the sum of entrance and exit burr heights with corresponding coefficients of determination (R^2) of 0.68 and 0.79 respectively. Conversely, the correlation for AA2024 was considerably weaker with a R^2 value of 0.54.

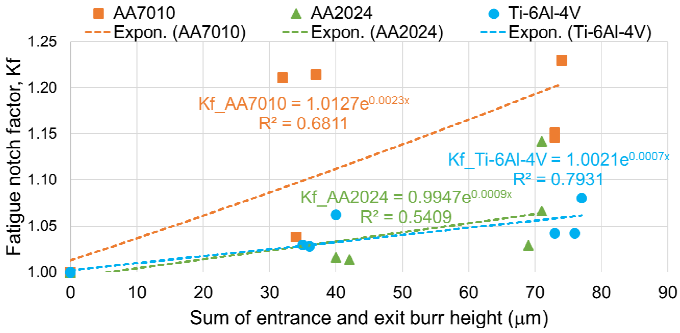

Fig. 10. Regression plots for fatigue notch factor against the sum of entrance and exit burr height.

Further analysis was performed by using burr volume instead of height as the characteristic notch dimension. The burrs were assumed to have a triangular cross section based on their respective height (BH) and width (BW), which is consistent around the hole diameter (d). Hence, the burr volume (BV) was approximated according to Eq (5).

$$BV = \pi d \left(\frac{BW \cdot BH}{2} \right) \tag{5}$$

Fig. 11 detail the regression plots for K_f versus the sum of the entrance and exit burr volume for each of the 3 workpiece materials. The correlation of K_f against the sum of burr volume was poorer compared to burr height, with R^2 values of 0.65, 0.43 and 0.72 for AA7010, AA2024 and Ti-6Al-4V respectively.

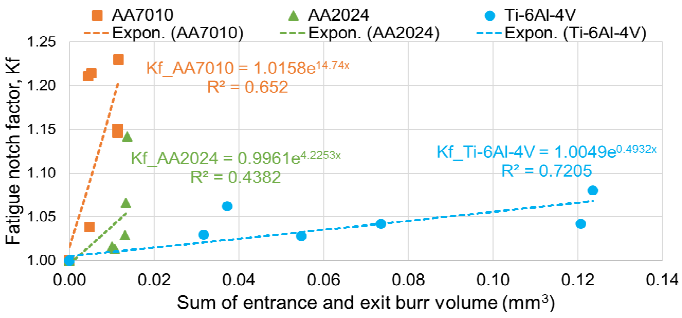

Fig. 11. Regression plots for fatigue notch factor against the sum of entrance and exit burr volume.

Results of the regression analysis highlighted that K_f generally increased with burr size, however the influence of hole diameter was not considered in the present investigation. It has been previously reported that the stress concentration induced by burrs and its effect on fatigue life diminished for specimens with larger diameter holes [9]. This suggests that the accuracy of fatigue notch factor estimation due to burr formation could potentially be improved by normalising the characteristic notch dimension (in this case the sum of burr heights) with respect to corresponding hole diameter (d), as proposed in Eq. (6);

$$K_{f|normalised} = c_1 e^{c_2 \frac{BH_{entrance} + BH_{exit}}{d}} \quad (6)$$

where c_1 and c_2 are constants depending on the workpiece material.

Determination of the empirical constants would require significant additional experimental work involving different workpiece specimens having a range of hole diameters with drilling operations at varying feed rates.

4. Conclusions

Burr formation was found to have a significant effect on the fatigue performance of drilled AA7010 and Ti-6Al-4V specimens, with deburring increasing the mean number of cycles to failure by up to 283% and 69% respectively. In contrast, the influence of burrs on failure appeared to be less dominant in the AA2024 samples, due possibly to the greater damage tolerance of the under-aged alloy. Fractography analysis of the AA2024 specimens revealed that fatigue cracks largely initiated on the drilled surfaces away from the entrance or exit of the holes. This was consistent with associated ANOVA results showing that hole condition was not a significant factor with regard to fatigue life. Conversely, the fatigue cracks in both the AA7010 and Ti-6Al-4V specimens principally originated in the vicinity of hole exit burrs. Reasonably good correlations were observed between K_f and the sum of entrance and exit burr heights for AA7010 and Ti-6Al-4V with R^2 of 0.68 to 0.79 respectively. In contrast, the corresponding correlation for AA2024 was relatively weak with R^2 of 0.54.

Acknowledgements

The authors wish to thank Airbus Operations Ltd., Mapal Ltd. and the University of Birmingham for the provision funding, workpiece materials, equipment, tooling and technical support. Thanks are due to Prof. Paul Bowen, Dr. Timothy Doel and David Price from the School of Metallurgy and Materials, University of Birmingham for granting access to the fatigue testing equipment and associated technical assistance. The authors are also grateful to Yamazaki Mazak UK Ltd. for providing the machine tool used for the drilling operations.

References

[1] Hale J (2006) Boeing 787 from the Ground Up. *Aero* 24(4):17-23.
[2] Kuo CL, Soo SL, Aspinwall DK, Carr C, Bradley S, M'Saoubi R, Leahy W (2018) Development of Single Step Drilling Technology for Multilayer Metallic-Composite Stacks using Uncoated and PVD Coated Carbide Tools. *Journal of Manufacturing Processes* 31:286-300.
[3] Everett Jr RA (2004) The Effect of Hole Quality on the Fatigue Life of 2024-T3 Aluminum Alloy Sheet. *NASA/TM-2004-212658 ARL-TR-3106,* Langley Research Center, Virginia.
[4] Ralph WC, Johnson WS, Makeev A, Newman Jr JC (2007) Fatigue Performance of Production-Quality Aircraft Fastener Holes. *International Journal of Fatigue* 29:1319-1327.
[5] Newman Jr JC, Johnson WS, Zhao W (2009) Assessment of Residual Stresses and Hole Quality on the Fatigue Behavior of Aircraft Structural Joints - Volume 1: Stress Analyses, Fatigue Tests, and Life Predictions *Technical Report DOT/FAA/AR-07/56,V1*, US Department of Transportation, Washington DC.
[6] Sun D, Keys D, Jin Y, Malinov S, Zhao Q, Qin X (2016) Hole-making and its Impact on the Fatigue Response of Ti-6Al-4V Alloy. *Procedia CIRP* 56:289-292.
[7] Koster WP, Kohls JB, Cammett JT, Cornell BL (1977) *Verification of Production Hole Quality – Volume I,* Defense Technical Information Center, Ft. Belvoir.
[8] Noronha PJ, Henslee SP, Gordon DE, Wolanski ZR, Yee BGW (1978) Fastener Hole Quality. *Technical Report AFFDL-TR- 78-206 - Vol. 1,* Air Force Wright Aeronautical Laboratories, Ohio.
[9] Nishimura T (2002) Fatigue Performance of Open Drilled Holes with Burrs. *Journal of Testing and Evaluation* 30(6):478-482.
[10] Lanciotti A, Polese C (2008) Fatigue Properties of Monolithic and Metal-Laminated Aluminium Open-Hole Specimens. *Fatigue and Fracture of Engineering Materials and Structures* 31:911-917
[11] Barter SA, Molent L, Wanhill RJH (2012) Typical Fatigue-Initiating Discontinuities in Metallic Aircraft Structures. *International Journal of Fatigue* 41:11-22.
[12] Abdelhafeez AM, Soo SL, Aspinwall DK, Dowson A, Arnold D (2015) Burr Formation and Hole Quality when Drilling Titanium and Aluminium Alloys. *Procedia CIRP* 37:230-235.
[13] Haritos GK, Nicholas T, Lanning DB (1999) Notch Size Effects in HCF Behavior of Ti-6Al-4V. *International Journal of Fatigue* 21(7):643-652.
[14] Carvalho ALM, Voorwald HJC (2007) Influence of Shot Peening and Hard Chromium Electroplating on the Fatigue Strength of 7050-T7451 Aluminum Alloy. *International Journal of Fatigue* 29(7):1282-1291.
[15] Kermanidis AT, Petroyiannis PV, Pantelakis SG (2005) Fatigue and Damage Tolerance Behaviour of Corroded 2024 T351 Aircraft Aluminum Alloy. *Theoretical and Applied Fracture Mechanics* 43(1):121-132.
[16] Alexopoulos ND, Migklis E, Stylianos A, Myriounis DP (2013) Fatigue Behavior of the Aeronautical Al-Li (2198) Aluminum Alloy under Constant Amplitude Loading. *International Journal of Fatigue* 56:95-105.
[17] Wei LW, De Los Rios ER, James MN (2002) Experimental Study and Modelling of Short Fatigue Crack Growth in Aluminium Alloy Al7010-T7451 under Random Loading. *International Journal of Fatigue* 24(9):963-975.
[18] Wanhill RJH (1994) Flight Simulation Fatigue Crack Growth Testing of Aluminium Alloys: Specific Issues and Guidelines. *International Journal of Fatigue* 16(2):99-110.
[19] Hawkyard M, Powell BE, Stephenson JM, McElhone M (1999) Fatigue Crack Growth from Simulated Flight Cycles Involving Superimposed Vibrations. *International Journal of Fatigue* 21:S59-S68.
[20] ASTM E466 (2015) *Conducting Force Controlled Constant Amplitude Axial Fatigue Tests of Metallic Materials*, ASTM International, USA.
[21] Suraratchai M, Limido J, Mabru C, Chieragatti R (2008) Modelling the Influence of Machined Surface Roughness on the Fatigue Life of Aluminium Alloy. *International Journal of Fatigue* 30:2119-2126.
[22] Dursun T, Soutis C (2014) Recent Developments in Advanced Aircraft Aluminium Alloys. *Materials and Design* 56:862-871.
[23] Campbell FC (2012) *Fatigue and Fracture: Understanding the Basics,* ASM International, Ohio.
[24] Suresh S (1998) *Fatigue of Materials, 2nd ed.* Cambridge University Press, Cambridge.
[25] Carter RD, Lee EW, Starke EA, Beevers CJ (1984) The Effect of Microstructure and Environment on Fatigue Crack Closure of 7475 Aluminum Alloy. *Metallurgical Transactions A* 15(3):555-563.
[26] Abdelhafeez AM, Soo SL, Aspinwall DK, Dowson A, Arnold D (2016) A Coupled Eularian Lagrangian Finite Element Model for Drilling Titanium and Aluminium Alloys. *SAE International Journal of Aerospace* 9(1):198-207.
[27] Stephens RI, Fatemi A, Stephens RR, Fuchs HO (2001) *Metal Fatigue in Engineering, 2nd ed.* John Wiley and Sons Inc., New York.
[28] Basquin OH (1910) The Exponential Law of Endurance Tests. *Proceedings of the American Society for Testing and Materials* 10(2):625-630.
[29] Pilkey WD, Pilkey DF (2008) *Petersen's Stress Concentration Factors, 3rd ed.* John Wiley and Sons Ltd, Chichester.